Supplemental Information

RAPGEF5 regulates nuclear translocation of β-catenin

John N. Griffin, Florencia del Viso, Anna R. Duncan, Andrew Robson, Woong Hwang, Saurabh Kulkarni, Karen J. Liu and Mustafa K. Khokha

Figure S1, Griffin et al.

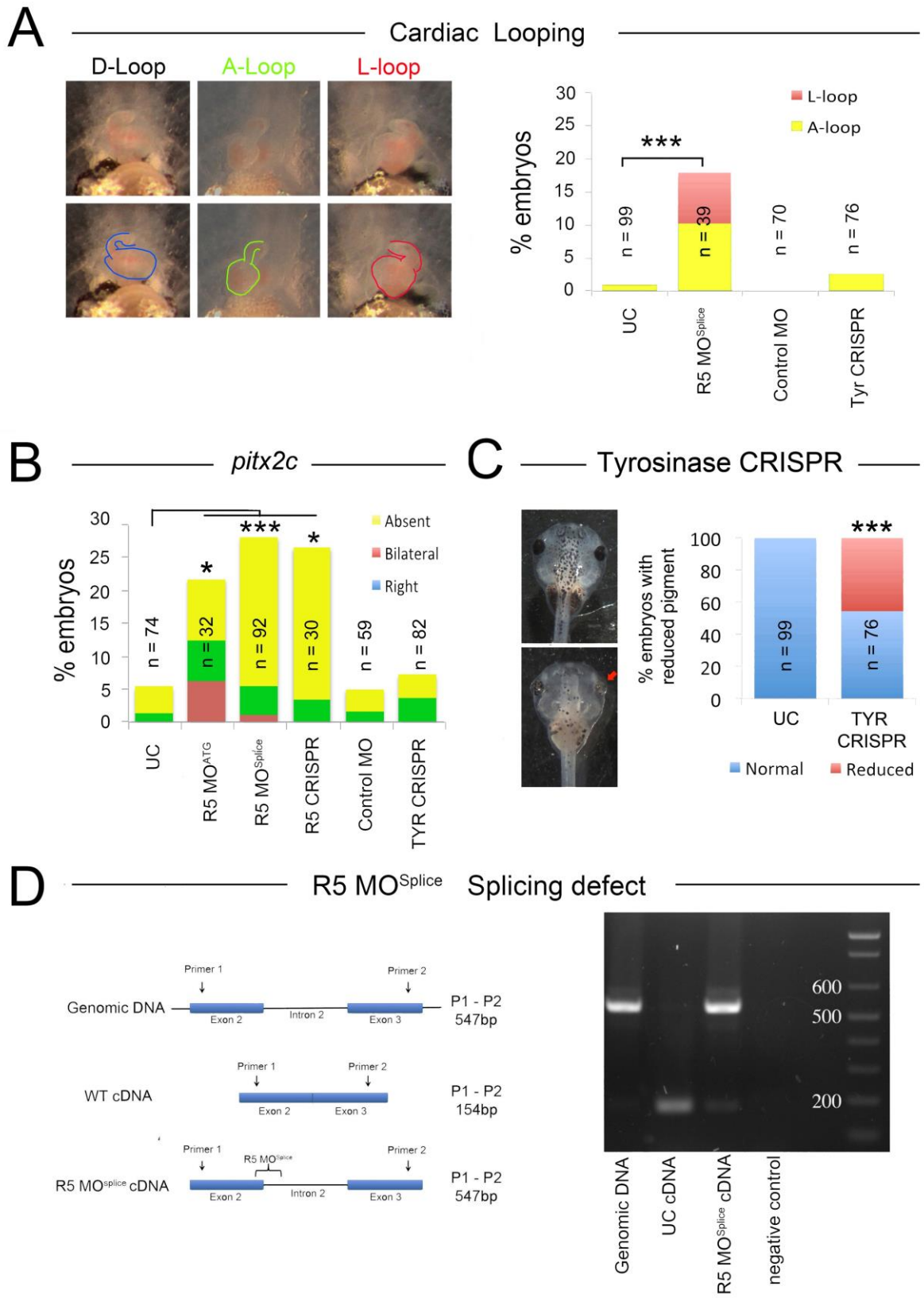

Figure S1. Related to Fig. 1; Depletion of Rapgef5. (A) Knockdown of Rapgef5 disrupts cardiac looping. Ventral views of *Xenopus* tadpoles with dorsal to the top. Representative examples of a normal (D-loop outlined in blue lower panel), and abnormal (A-Loop outlined in green, L-Loop outlined in red) looped heart. Injection of a control MO or a control CRISPR (targeting *tyrosinase*) does not affect cardiac looping. (B) Injection of a control MO or control CRISPR (targeting *tyrosinase*) does not cause abnormalities in *pitx2c* expression. (C) The control (*tyrosinase*) CRISPR reduces pigments levels in stage 45 *Xenopus* embryos, demonstrating that the control CRISPR/CAS9 system functions as expected. (D) Rationale of R5 MO^{Splice} design. The splice MO targets the splice donor site at the start of intron 2. Failure to excise intron 2 results in a premature stop codon early in the Rapgef5 protein. RT-PCR confirms that R5 MO^{Splice} causes retention of intron 2. In genomic DNA, intron 2 spanning primers amplify a band of 547bp. In WT cDNA, these primers amplify a band of 157bp. PCR primers amplifying cDNA from R5 MO^{Splice} morphants generate a band at 547bp indicating retention of intron 2 in mRNA. A “no template” negative control is also included. A single asterisk indicates $P<0.05$ and a triple asterisk $P<0.005$.

Figure S2, Griffin et al.

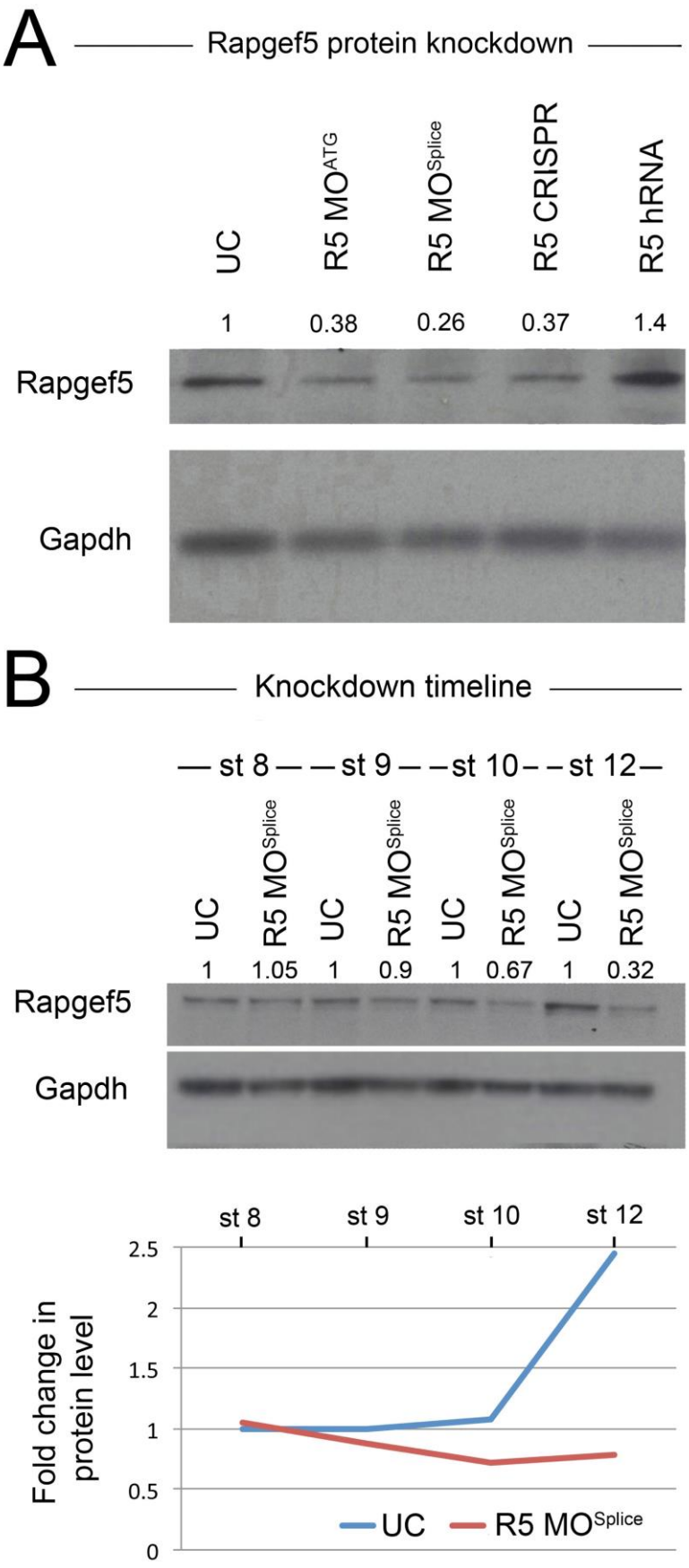

Figure S2. Related to Fig. 1; Depletion of Rapgef5 protein. (A) Western blot demonstrating the efficacy of the R5 MO^{ATG}, R5 MO^{Splice}, and CRISPR mediated Rapgef5 depletion in stage 10 *Xenopus* embryos. Overexpression of human RAPGEF5 mRNA increases protein levels. (B) Timeline of Rapgef5 depletion. Rapgef5 protein levels were unaltered in morphants at late blastula stages (st 8 and 9) but reduced at stage 10 and 12. The graph represents fold changes in Rapgef5 protein levels in control and depleted embryos relative to the stage 8 uninjected controls.

Figure S3, Griffin et al.

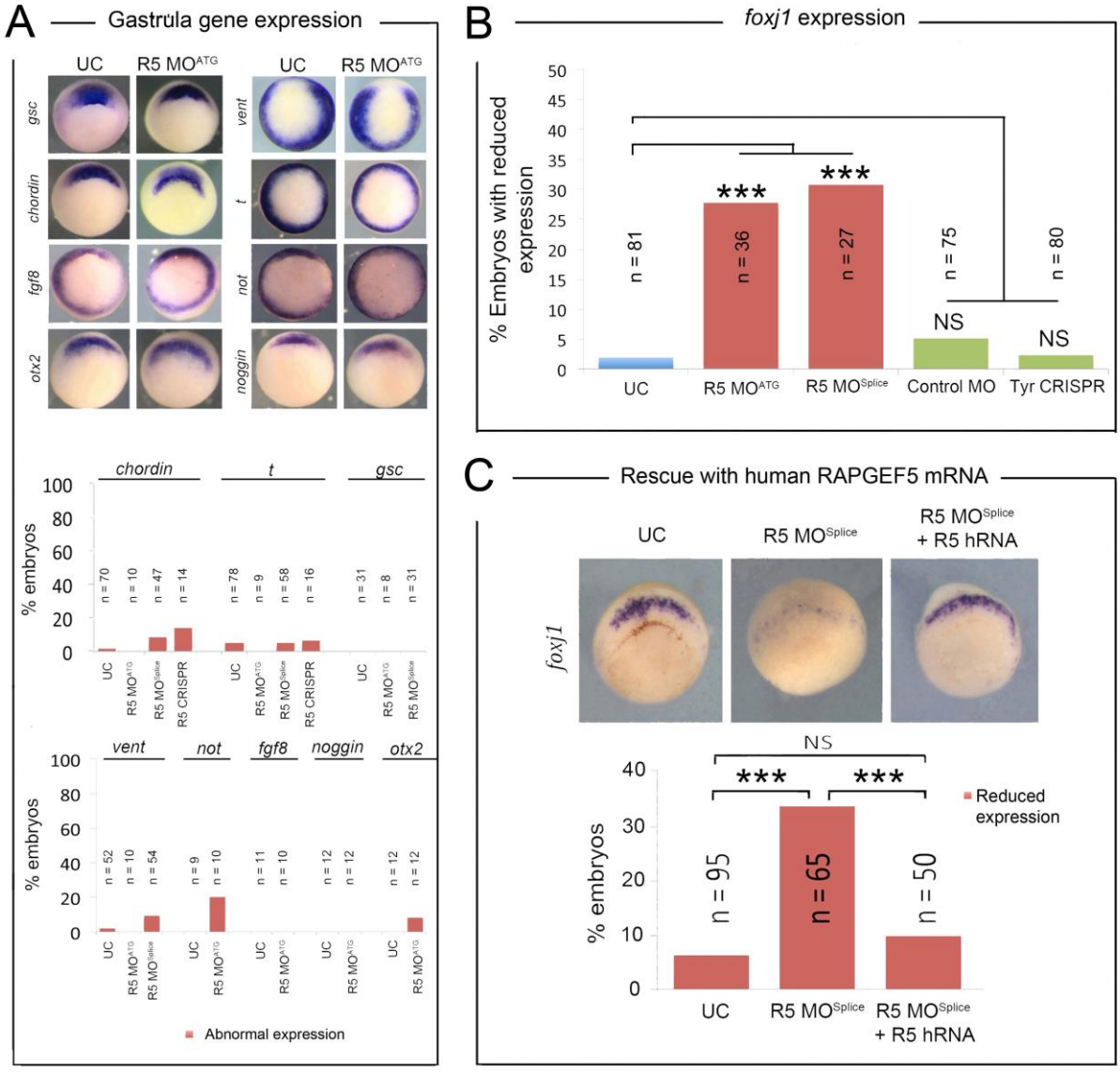

Figure S3. Related to Fig. 2; Expression of gastrulation genes in *rapgef5* morphants. (A) At stage 10, expression of numerous gastrulation markers (*gsc, chordin, fgf8, otx2, vent, t, not* and *noggin*) are less affected by depletion of Rapgef5 compared to *foxj1* or *xnr3* (See Fig. 2A). Vegetal views with dorsal to the top. (B) Injection of a control MO or a control CRISPR (targeting *tyrosinase*) does not affect *foxj1* expression (C) Co-injection of human *RAPGEF5* mRNA can rescue the loss of *foxj1* expression in *Rapgef5* morphants, demonstrating the specificity of the MO. Triple asterisks indicate P<0.005.

Figure S4, Griffin et al.

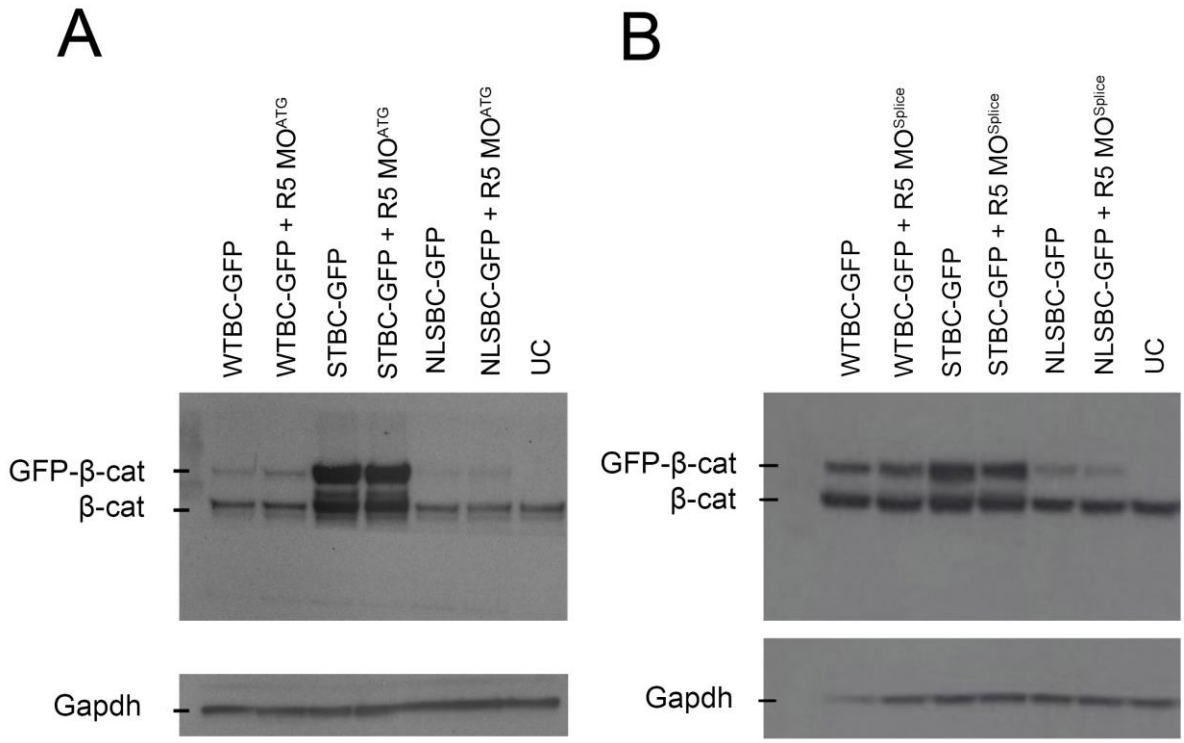

Figure S4. Related to Fig. 4 Translation of injected GFP tagged *β-catenin* mRNAs. Depletion of Rapgef5 by (A) ATG or (B) Splice MOs did not significantly affect translation of GFP tagged WT, ST, or NLS *β-catenin* mRNAs compared to controls.

Figure S5, Griffin et al.

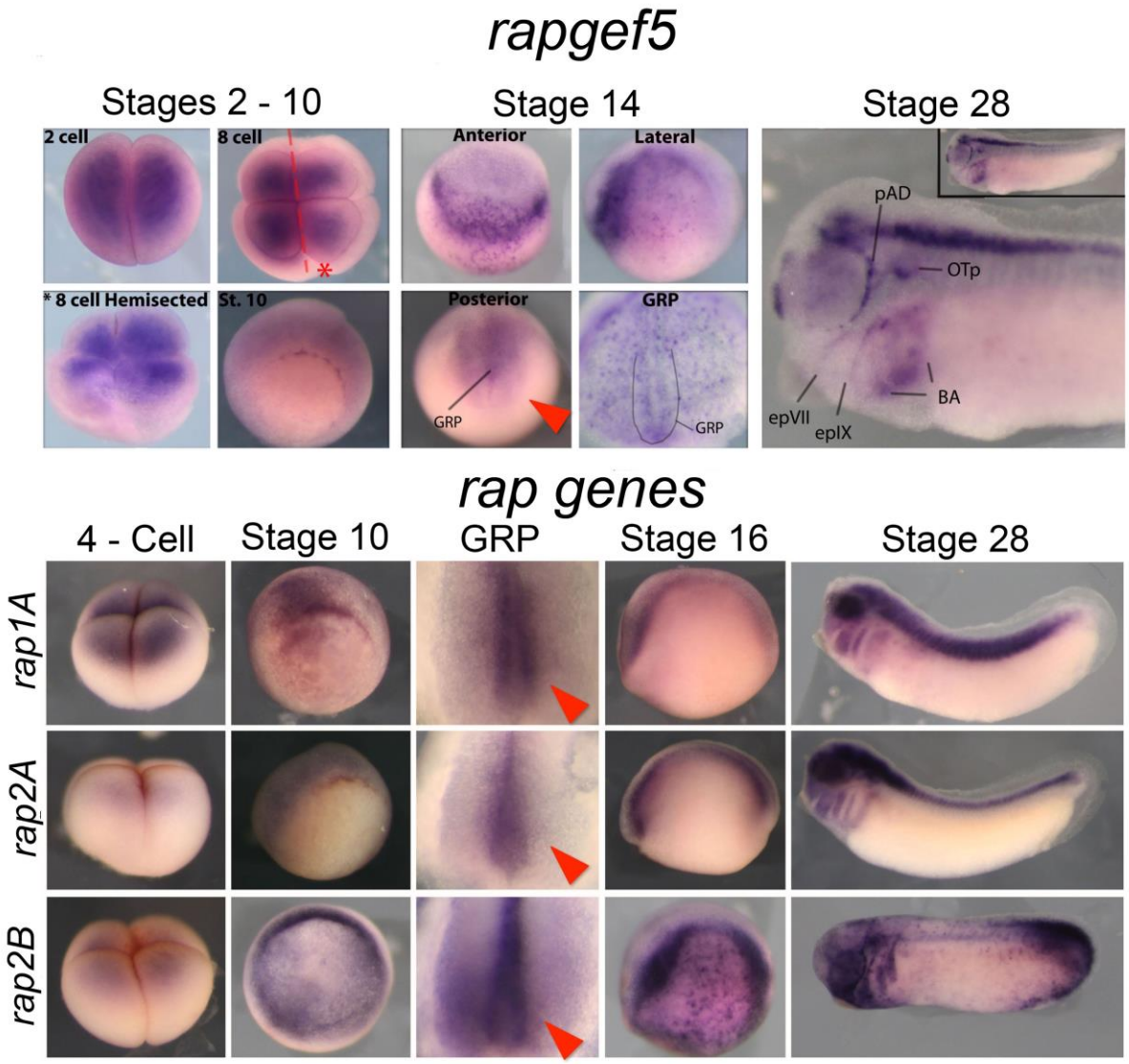

Figure S5. Related to Fig. 6; Developmental expression of Rapgef5 and Rap genes. *In situ* hybridization reveals *rapgef5* mRNA is present from the earliest stages of development. It is detected in the animal pole at the 2 cell and 8 cell stages. In the stage 10 embryos expression appears diffuse around the blastopore. At stage 14 transcripts are detected in the anterior neural folds and forming GRP. *rapgef5* expression is restricted to the anterior neural tube, brain, pharyngeal arches and cranial placodes at stage 28. Rap1A, Rap2A and Rap2B are all expressed in the 4 cell embryo, in the gastrulating stage 10 embryo and in the GRP at stage 16. Expression of all three genes is also strong in the neural folds at stage 16, while Rap2B also displays a speckled pattern on the lateral ectoderm. All three are expressed in the neural tube, brain, eye and pharyngeal arches at stage 28.

Figure S6, Griffin et al.

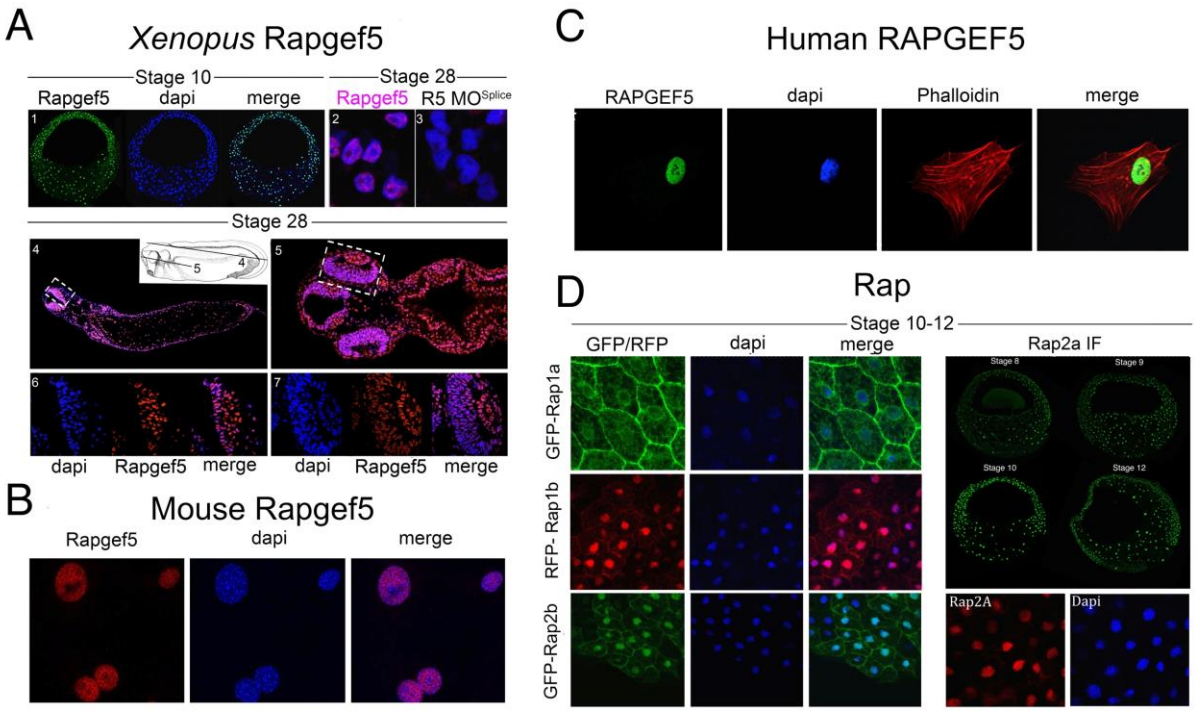

Figure S6. Related to Fig. 6; The subcellular localization of Rapgef5 and Rap proteins. (A1) Rapgef5 is localized to the nuclei in a section of a stage 10 *Xenopus* embryo. (A2 - 7) Rapgef5 is detected specifically in the nuclei of sectioned paraffin embedded stage 28 *Xenopus* embryos but is reduced in morphants (Compare A2 and A3, magenta Rapgef5, blue DAPI). The lines on the schematic in A4 represent the plane of section shown in A4 and A5. A6 and A7 are higher magnification of the white boxes in A4 and A5, respectively. (B, C) Rapgef5 localizes specifically to the nuclei of mouse MEFs and human RPE cells. (D) With the exception of Rap1A all rap proteins localize both to the plasma membrane and nucleus as assayed by injection of GFP/RFP tagged constructs or by immunofluorescence.

Figure S7, Griffin et al.

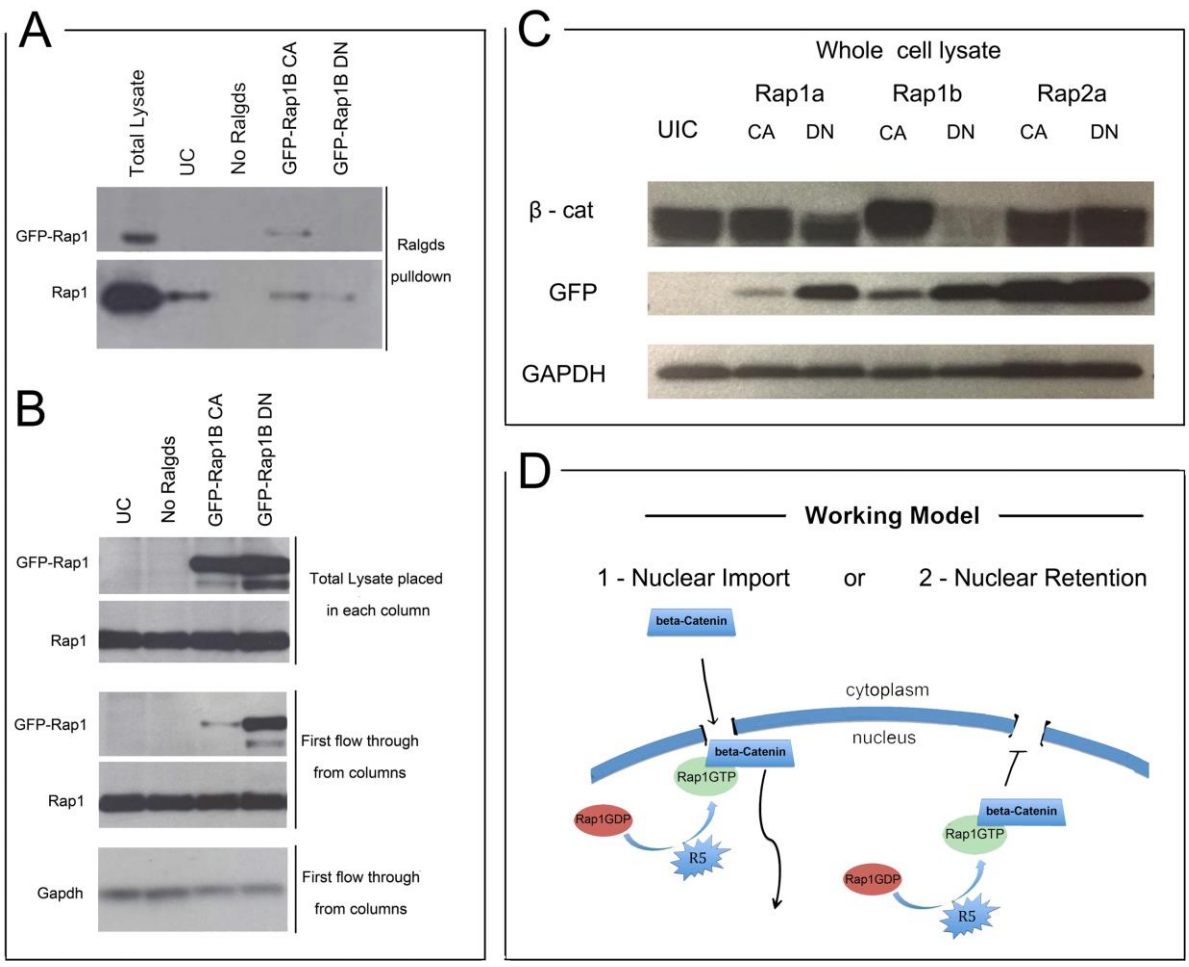

Figure S7. Related to Fig. 7; A Rap1 mediated transport system. (A) Validation of the CA (constitutively active) and DN (dominant negative) Rap1 constructs. ^{RBD}RalGDS selectively pulls down endogenous active RAPs, as well as the GFP tagged CA, but not the DN Rap1b mutant. (B) While the GFP tagged CA and DN Rap1 constructs can be equally detected in the total lysate, the level of the CA form is greatly reduced in the first flow through from the pull down columns, reflecting the binding of CA Rap1 to ^{RBD}RalGDS and its retention in the column. (C) Injection of CA Rap1a or Rap1b leads to an increase in total β-catenin protein levels relative to controls, while injection of the DN forms causes a decrease in total β-catenin levels. Injection of Rap2a CA or DN did not reveal a differential effect on β-catenin. (D) Proposed model for Rapgef5s role in nuclear localization of β-catenin. Rapgef5 maintains nuclear Raps in their active GTP bound confirmation, which is required for 1) – the nuclear import of β-catenin or 2) – retention of β-catenin within the nuclear compartment.